JACS
JOURNAL OF THE AMERICAN CHEMICAL SOCIETY
pubs.acs.org/JACS

Article

Catalysis in Extreme Field Environments: A Case Study of Strongly Ionized SiO_2 Nanoparticle Surfaces

Thomas M. Linker,* Ritika Dagar, Alexandra Feinberg, Samuel Sahel-Schackis, Ken-ichi Nomura, Aiichiro Nakano, Fuyuki Shimojo, Priya Vashishta, Uwe Bergmann, Matthias F. Kling,* and Adam M. Summers*

Cite This: J. Am. Chem. Soc. 2024, 146, 27563−27570

Read Online

ACCESS | Metrics & More | Article Recommendations | Supporting Information

ABSTRACT: High electric fields can significantly alter catalytic environments and the resultant chemical processes. Such fields arise naturally in biological systems but can also be artificially induced through localized nanoscale excitations. Recently, strong field excitation of dielectric nanoparticles has emerged as an avenue for studying catalysis in highly ionized environments, producing extreme electric fields. While the dynamics of laser-driven surface ion emission has been extensively explored, understanding the molecular dynamics leading to fragmentation has remained elusive. Here, we employ a multiscale approach performing nonadiabatic quantum molecular dynamics (NAQMD) simulations on hydrogenated silica surfaces in both bare and wetted environments under field conditions mimicking those of an ionized nanoparticle. Our findings indicate that hole localization drives fragmentation dynamics, leading to surface silanol dissociation within 50 fs and charge transfer-induced water splitting in wetted environments within 150 fs. Further insight into such ultrafast mechanisms is critical for the advancement of catalysis on the surface of charged nanosystems.

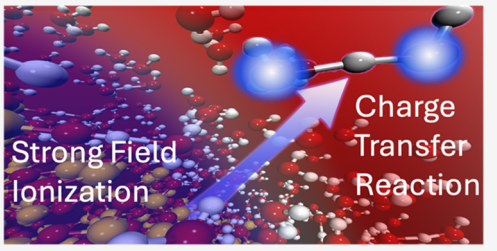

INTRODUCTION

The influence of electric fields on molecular and electronic structures has been a subject of scientific inquiry since the pioneering work of Stark, who over a century ago documented field-induced shifts in electronic energy levels.[1] Recent research has expanded our understanding of how electric fields affect chemical bonding with significant insights into their role in driving localized bond breaking only emerging in the past few decades.[2−4] Notably, extreme electric fields have been known to emerge from local gradients/dipolar structures in biological systems, with magnitudes up to ∼1 V/Å.[5] However, the role of these fields in catalysis reactions has only relatively recently come to light.[6−9] Rare reaction channels, such as water autoprotolysis ($2H_2O \rightarrow H_3O^+ + OH^-$), have been attributed to spontaneous dipolar arrangements that lead to the generation of large local electric fields (reaching magnitudes of up to 3 V/Å), underscoring the potential of strong local electric fields to drive unique chemical dynamics.[10−12]

Building upon these principles, recent advancements in catalysis and efforts to drive increases in catalytic rates have sought to harness strong local electric fields, generated through both direct methods such as scanning tunneling microscopes (STM) as well as indirect methods through the creation of chemical environments with strong local electric fields.[13−15] Engineering of catalytic processes is pivotal in various industrial and environmental applications, including energy conversion, pollution mitigation, synthesis of fine chemicals, and even cancer treatments.[16−21]

Another direct method to generate strong local electric fields is light manipulation of nanoparticles, which can generate ionized particle surfaces with correspondingly strong electric fields. Historically, photocatalysis at nanoscale has focused on localized surface plasmon resonance (LSPR) in metal nanoparticles and has been predominantly associated with noble-metal nanoparticles, such as gold and silver, which exhibit strong LSPR in the visible spectrum.[18] However, the inherent energy losses and non-negligible heat generation associated with these materials under laser excitation have prompted the exploration of alternative platforms. Dielectric nanoparticles, such as silica, have been proposed as an energy-efficient alternative, capable of inducing catalytic reactions through mechanisms like strong field ionization without the drawback of excessive thermal effects.[22] Recent advancements have highlighted the induction of catalytic reactions on silica nanoparticles through strong field ionization, leading to the generation of free charges that instigate a cascade of chemical dynamics.[23−29] Notably, the formation of trihydrogen cations

Received: June 24, 2024
Revised: September 16, 2024
Accepted: September 17, 2024
Published: September 27, 2024

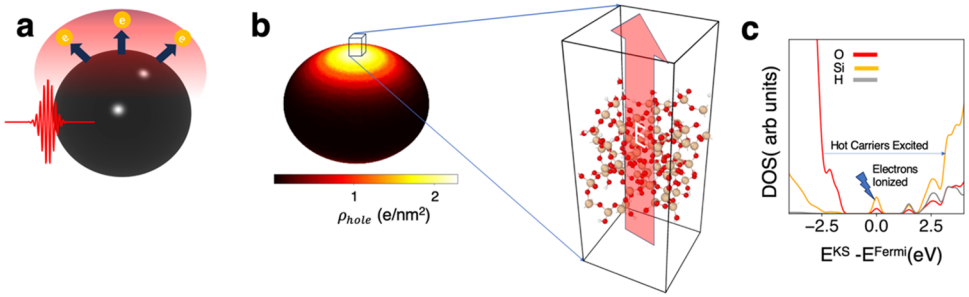

Figure 1. (a) Diagram of strong field-induced electronic ionization. Due to near-field enhancement of the ionizing laser, the density of ionized electrons is much higher at the poles. (b) Resultant nonuniform charge density on the nanosphere from ionization from the optical pump pulse. This ionization density creates a strong electric field on the surface of the nanosphere. We use the range of electric field strengths on the surface of the sphere as boundary conditions for nonadiabatic quantum molecular dynamics (NAQMD) simulations on a model amorphous silica surface slab. Si atoms are colored tan, oxygen red, and hydrogen white. (c) Element-projected Kohn−Sham (KS) density of states of the model amorphous silica slab with relevant excitations indicated.

(H_3^+) from the dissociation of molecular adsorbates on silica surfaces has been demonstrated, unveiling a novel inorganic pathway for H_3^+ formation.[25] H_3^+ serves as a hallmark for water splitting and as a precursor for forming complex organic compounds.[30] Understanding the pathways that give rise to trihydrogen cations and similar reaction channels can not only give insight into the use of strong field excitation as a method for photocatalysis but also elucidate the general chemistry in extreme field conditions. The strong field excitation creates not only free charge carriers that directly partake in molecular fragmentation but also extreme electric field conditions on the surface of the nanoparticle. As up to tens of thousands of electrons can be ejected from nanoparticles upon strong field ionization, local fields reaching ∼1 V/Å can be achieved at the particle surface.[23−29] Since silica is largely noncatalytic prior to ultrafast laser excitation, the ability to rapidly induce strong and highly localized electric fields allows for controllable and time-resolved studies of the mechanisms for catalysis in such strong fields with free charge carriers.

Despite the recent progress, understanding the precise role that surface charges and local fields play on the dynamics of chemical bonding and the ultrafast time scales on which these interactions occur in nanoscale systems has remained elusive. Here, we adopt a multiscale simulation approach to investigate the molecular fragmentation dynamics resulting from strong field ionization of wetted silica nanosurfaces. The multiscale approach is needed as first-principles molecular simulations based on density functional theory (DFT) can at most simulate a few thousand atoms, while typical nanoparticles used in experiments exceed 25 nm and thus contain millions of atoms or more. While the simulations presented here are performed for ionized silica nanoparticles, the mechanisms and time scales uncovered for molecular fragmentation dynamics are anticipated to be relevant to many avenues of catalysis in strong field environments with free charge carriers.

METHODS

In the first step of this multiscale approach, we calculate the electric field formed on the ionized silica surface. We first compute the hole/charge distribution generated on the surface of a nanosphere through strong field ionization from a typical ultrashort 800 nm, 5 fs laser pulse. Further information on these strong field ionization simulations can be found in Supporting Information (SI). These conditions are very similar to those reported in previous experimental studies on the strong field ionization of nanoparticles.[23−29] Due to near-field enhancement effects from the Mie scattering of the laser pulse with the nanosphere and the nonlinear nature of strong field ionization, the distribution is nonuniform with a high concentration of ions at the poles of the sphere. A diagram of this process is illustrated in Figure 1a. While the initial conditions were chosen to resemble previous experimental work, the results discussed below apply more broadly to other charge distributions on nanosurfaces.

Figure 1b shows the positive (hole) charge density formed on the surface of a silica sphere with a 50 nm radius within 5 fs duration for a laser pulse with 5×10^{13} W/cm^2 intensity. The density ranges up to ∼2.5 ionized electrons per square nanometer. These values are consistent with measured electron emissions for strong field excitations and are in the range of hole concentrations we explored in this study. More details of how this density is computed are described in the SI (see Figures S1 and S2). The ionization rate, and thus the surface charge density is maximized at the poles and falls off with polar angle. Within this 5 fs window, the atoms on the surface have experienced little motion and are now exposed to an extremely strong electric field resulting from the positive charge distribution on the particle surface. This is the starting point for our molecular simulations, where we use the range of electric field strengths on the nanosphere surface as field boundary conditions for a small ∼1 nm^2 amorphous hydrogen-terminated silica slab. The amorphous slab is visualized in Figure 1b. We find that the largest magnitude of the field at any point on this surface is on the order of ∼2 V/Å and the lowest on the order of 0.2 V/Å (see Figure S2). The local fields are consistent with what is anticipated from electron emission measurements.[26]

Thus, to understand the molecular fragmentation dynamics, NAQMD simulations[31,32] in the presence of a static electric field are performed on a small ∼1 nm^2 hydrogen-terminated amorphous silica surface. The application of a strong DC field along an amorphous silica surface to model the effect of the fields induced by the global hole density on the nanosphere is similar to globally informed Hartree potential frameworks in divide and conquer density functional theory.[33] Our ADK simulations indicate the distribution of electric field magnitude on the surface of the sphere ranges from ∼0.2 to 2 V/Å, so we investigate fields within this range (see Figure S2). NAQMD simulations are based on time-dependent DFT (TD-DFT) within the surface hopping approach.[34] Calculations are performed on a plane-wave basis with the projected augmented wavevector (PAW) method.[35] The Perdew−Burke−Ernzerhof (PBE) version of generalized gradient approximation (GGA)[36] was used and van der Waals corrections were employed utilizing the DFT-D scheme[37] (further details are given in the SI). We consider the ionization of electrons as well as the high-energy electron−hole pairs (i.e., nonionizing excitations) which can occur due to local Coulomb trapping.[26] Excitation is modeled as an instantaneous excitation of electrons from the valence bands determined from the ground-state electronic structure. As typical laser pulses used in experiments to investigate ultrafast, strong field chemistry in nanosystems are quite short (∼5 fs pulse duration), this prompt excitation approximation is reasonable.

https://doi.org/10.1021/jacs.4c08550
J. Am. Chem. Soc. 2024, 146, 27563−27570

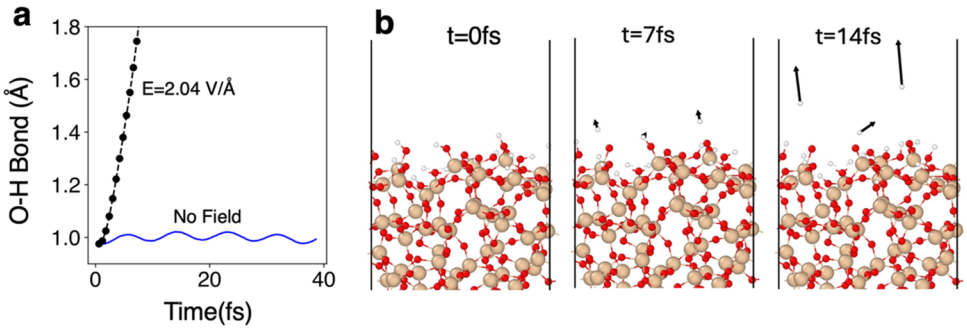

Figure 2. (a) O−H bond dynamics for surface selected silanol group in the presence of a large electric field where ultrafast dissociation was seen. (b) Snapshots of MD trajectory under strong electric field with arrows drawn for protons quickly escaping the surface.

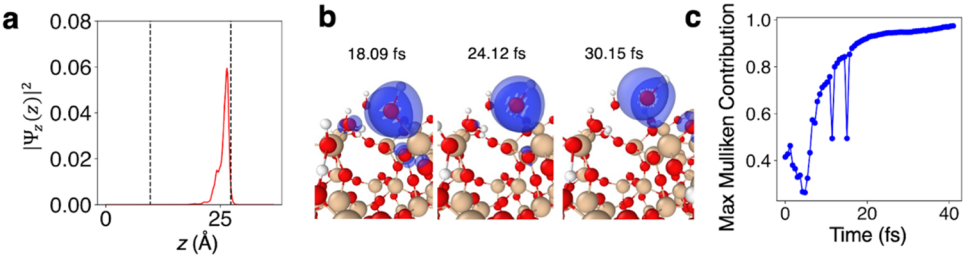

Figure 3. (a) Initially excited VBM wave function at 0.71 V/Å. Wave function is primarily localized to the atomically thin surface layer. (b) Dissociation dynamics at 0.71 V/Å. Localization of hole (blue isosurface) to single oxygen atom on silanol group results in breaking of Si−O bond and formation of OH^+. (c) Localization dynamics of the hole wave function as a function of time quantified by the maximum Mulliken population of any given atom to the hole wave function. A value of 1 indicates complete localization.

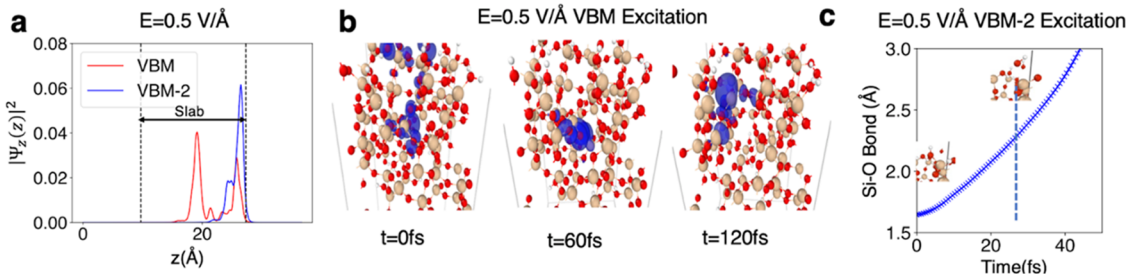

Figure 4. (a) VBM and VBM-2 wave functions for an electric field of 0.5 V/Å. VBM-2 shows primarily surface localization, while the VBM is hybridized between the surface and the bulk. (b) Hybridized surface-bulk VBM excitation breaks SiO_4 tetrahedra, resulting in fast diffusion of the SiO_3^+ complex within the bulk of the slab. (c) Surface VBM-2 excitation results in rapid breaking of the Si−OH bond.

Partial densities of states projected onto elements (O, Si, and H) are also plotted for the amorphous silica slab in Figure 1c with relevant excitations illustrated. In the amorphous slab, a gap state is formed at the Fermi level. This is expected to occur in wetted silica slabs with dangling bonds.[38,39]

RESULTS

We first examined the effects of the largest field strengths on the surface of the nanosphere. When the electric field is on the order of ∼2 V/Å, the dissociation of O−H bonds at the surface is nearly instantaneous (<∼10 fs) regardless of whether any local charge carriers are present. Figure 2a illustrates the dynamics of the O−H bond at the hydrogen-terminated silica surface under a 2 V/Å field for a given O−H bond on the surface compared to the ground-state dynamics, for which ultrafast dissociation can be seen. Snapshots of the MD trajectory are shown in Figure 2b where within 24 fs three protons are ejected. For such strongly ionized surfaces and their corresponding strong electric fields, the dynamics are essentially limited by the O−H stretching frequency.

At a weaker field strength close to 1 V/Å, we found that the dynamics become more subtle and are highly dependent on the spatial distribution of the excitation as well as the local hole density. In this regime, we first considered the local field dependence for a region with a high distribution of excited carriers with the valence band being doubly excited to a high-lying electronic state and the gap state empty (three holes and two excited electrons, net ionization state of +1). For these simulations, we found that the excited electrons were highly delocalized and did not contribute to the dissociation dynamics beyond thermalization from carrier-phonon scattering, and all dissociation dynamics was driven by the holes. We also investigated higher net charge states with and without excited electrons and found similar results (see Figures S3 and S4). At investigated field strengths of 1.02 and 0.71 V/Å, we found the VBM would be primarily localized on the surface of the slab with the z dependence for the VBM wave function for a field of 0.71 V/Å strength illustrated in Figure 3a. Figure 3b shows the dynamics for an excitation from this state resulting in the excited hole wave function quickly localizing to an

https://doi.org/10.1021/jacs.4c08550
J. Am. Chem. Soc. 2024, 146, 27563−27570

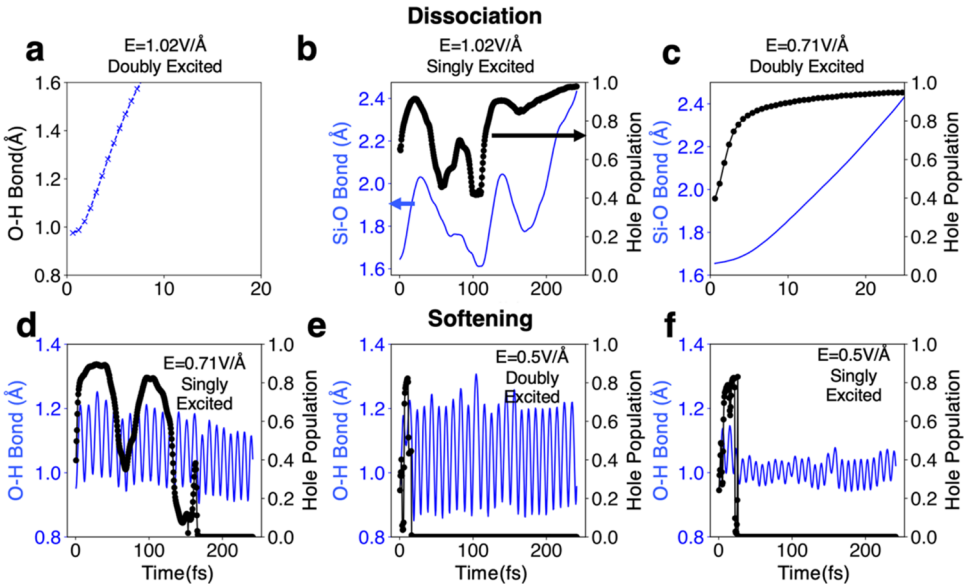

Figure 5. (a) Ultrafast dissociation of the O−H bond in the doubly excited surface valence state with a filled gap state and electric field of 1.02 V/Å. (b) Same conditions as (a) but singly excited valence state. This results in a much longer dissociation process of a surface silanol group bond, resulting in OH^+. Long dissociation process is a result of long hole localization time. (c) Same conditions as (a) but lower field of 0.71 V/Å resulting in ultrafast dissociation of the Si−OH bond resulting in OH^+. Similar to the dynamics observed with gap state unoccupied, as described in Figure 3. (d) Same conditions as (c) but singly excited state resulting in softening of the O−H bond with long period of hole localization. O−H bond dynamics slowly relax after the hole localizes to the bulk. (e) Same conditions as (a) but lower field of 0.5 V/Å. Brief hole localization on a surface O atom results in O−H bond softening. The O−H bond remains softened well after the hole wave function localizes to the surface. (f) Same conditions as (e) but singly excited hole wave functions. Brief hole localization slightly disturbs O−H bond dynamics before relaxing back to near-ground-state vibrational stretching.

individual oxygen atom. This results in the dissociation of the Si−O bond and the formation of an OH^+ ion within 30 fs. The localization dynamics of the VBM wave function is plotted in Figure 3c, showing the maximum Mulliken population of any given atom for the VBM wave function as a function of time. Here, the value of unity indicates that the VBM wave function is entirely localized to one atom. Figure 3c illustrates that localization of the VBM wave function is crucial to dissociation. Such localization has similarly been proposed as the rate-limiting step in strong field dissociation of water.[42], It was found that the gap state hole was primarily localized to bare O and Si atoms and did not contribute to any dissociation (see Figure S5 in the SI), indicating that such states while contributing to the overall global charge state of the ionized nanosphere can locally suppress dissociation by trapping carriers that would otherwise contribute to bond breaking.

In fields below 0.71 V/Å, we found that the VBM was not initially localized to surface atoms but primarily localized to the bulk of the slab, with the z dependence of the VBM probability distribution plotted in Figure 4a for an electric field of 0.5 V/Å. We found that under these conditions, the dynamics would not result in fast bond dissociation (<100 fs). Here, the holes would primarily localize to a SiO_4 tetrahedron in the center of the slab, resulting in fast diffusion of these atoms. Figure 4b shows the initial atomic configuration with the VBM wave function hybridized between the surface and the bulk atoms. The excited VBM hole wave function then eventually localizes to SiO_4 tetrahedra within the center slab, resulting in the tetrahedra breaking as illustrated in Figure 4b. We observed similar dynamics when exciting from a bulk-like valence state with a field strength of 0.71 V/Å, which are illustrated in Figure S6.

Since the difference between the VBM, VBM-1, and VBM-2 energies was less than 100 meV, we also considered excitations from these states if the initial wave functions were more localized to surface atoms. The z dependence of the VBM-2 wave function for a field of 0.5 V/Å is illustrated in Figure 4a, which is localized to the surface of the slab. We found down to a field of 0.5 V/Å that when excited from a surface localized state, Si−OH disassociation would occur within 30 fs, with dynamics plotted in Figure 4c. The dissociation for fields of 1.02, 0.71, and 0.5 V/Å was found to be on the order of 30 fs for a surface-like excitation. Below the 0.5 V/Å field, we did not observe any dissociation within 240 fs of simulation.

The difference in dynamics due to the spatial extent of the excited holes can be thought of in terms of Wannier-Stark localization of the electronic states to lattice sites in the presence of an electric field.[42−44] In the case of holes with strong bulk-like character, this will localize them within the SiO_4 tetrahedra in the center of the slab. The field will still drive the holes to the surface of the slab but they are localized to the tetrahedra. As the deposited kinetic energy on the SiO_4 tetrahedra is not enough to overcome the collision barrier of the Si−O bonding network at the surface, this will result in rapid diffusion and collisions of the hole-localized SiO_4 tetrahedra.

Next, we examined the effect of decreasing the carrier concentration at the examined fields, by first filling the gap state and then decreasing the double valence excitation to a single excitation. The excitations were taken from wave functions near the valence edge that were localized to the surface. For a field strength of 1.02 V/Å, we found that ultrafast dissociation still occurred with a double valence excitation and the gap state filled, with fast proton ejection observed within 10 fs as illustrated in Figure 5a. For a single

https://doi.org/10.1021/jacs.4c08550
J. Am. Chem. Soc. 2024, 146, 27563−27570

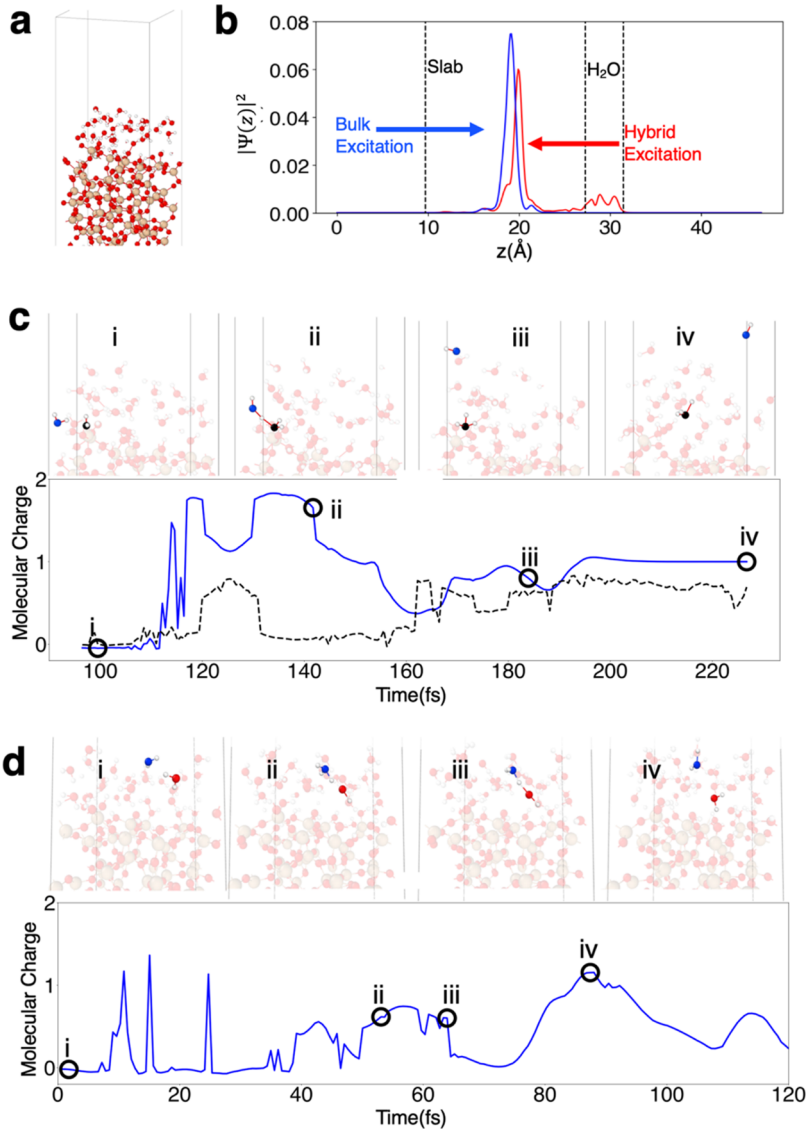

Figure 6. (a) Simulated silica water interface. Periodic boundary box shown with white lines. (b) Initial hole wave functions excited spatial distributions. (c) Molecular snapshots and local charges computed via Mulliken analysis for two water molecules that undergo water splitting reaction for hybrid excitation. Labeled points on the plot correspond to snapshots of the molecular dynamics trajectory plotted above during the formation and splitting of H_2O^{2+} to form OH^+ and H_3O^+ fragments. (d) Molecular snapshots and local charges computed via Mulliken analysis for a water molecule that undergoes hole localization, splitting, and recombination during the simulation for bulk-like excitation. Labeled points correspond to snapshots from the MD simulation plotted above illustrating the dissociation, recombination, and ejection of the water molecule from the surface.

excitation, we found a much longer dissociation process, with Si−OH dissociation occurring within 220 fs, as illustrated in Figure 5b. The long dissociation process was a result of the long localization time of the hole wave function to a surface oxygen atom. During this time, the periods of partial hole localization to the surface oxygen atom involved in the dissociation process led to softening of the Si−O bonds as well as the O−H bond involved in the dissociating silanol group (see Figure S7 in the SI).

When reducing the field to 0.71 V/Å and doubly exciting a surface valence wave function, we saw an ultrafast dissociation process within ∼20 fs, as illustrated in Figure 5c. This is similar to the case when doubly exciting with an unoccupied gap state. In contrast, when the same valence state was singly excited, we did not observe any dissociation. We found the hole wave function would begin with its maximum Mulliken population on a surface oxygen atom before eventually localizing to the bulk in ∼100 fs, which is illustrated in Figure 5d. This brief period on the surface oxygen atom resulted in a long period of softening and slow relaxation of the corresponding O−H stretching vibration due to the deposited kinetic energy from the localization period, as shown in Figure 5d. At a field strength of 0.5 V/Å, we saw similar softening dynamics without dissociation as a result of brief hole surface localization when doubly exciting a surface valence electron, as illustrated in Figure 5e. In contrast, when the gap state was unoccupied, the same double excitation led to ultrafast dissociation. This indicates that while the gap state we have found localizes to bare O and Si atoms at the surface and not the silanol groups, it can still contribute to silanol dissociation through its interaction with other holes. When only singly excited, a similar brief hole localization only led to brief elongation of the

https://doi.org/10.1021/jacs.4c08550
J. Am. Chem. Soc. 2024, 146, 27563−27570

O−H bond before relaxing to near-ground-state stretching dynamics as illustrated in Figure 5f (see Figure S7 for an example of ground-state stretching dynamics).

Overall, these results indicate that for a wetted silica surface, a threshold behavior for ultrafast dissociation occurs in terms of both local charge density and the global charge state. Such threshold-like behavior has similarly been observed in charge localization and resulting bond dissociation i dielectric breakdown.[45] We note these simulations cannot capture large spatiotemporal dynamics, and effects such as electron−hole recombination and charge diffusion are also anticipated to play a role. However, the results clearly show the necessity for surface charge localization to initiate fragmentation on bare silanol groups. In addition, in weaker excitation regimes, brief periods of surface localization on surface oxygen atoms result in substantial softening of affected O−H bonds, which can lead to fragmentation if they interact with other surface molecules.

Next, we examined the dynamics in a wetted environment with free water molecules present on the surface. Figure 6a shows the amorphous silica surface with 27 water molecules deposited on top. As we found that excitations within the bulk of the bare slab would not result in fast dissociation processes, we considered both excitations from the bulk of the slab and those hybridized with the surface water molecules with their spatial profiles plotted in Figure 6b. In both cases, we considered an excitation condition (E = 0.5 V/Å, doubly excited valence excitation, and empty gap state) where in the bare slab case, the spatial dependence of the excited hole wave function determined if molecular fragmentation occurred. The gap state was again not found to contribute to dissociation. We found that in both excitation cases, the holes transfer from silica to free water molecules resulting in water splitting events. For the hybrid-like excitation, we found that the two holes would localize on a single water molecule, resulting in a $H_2O^{2+} + H_2O \rightarrow OH^+ + H_3O^+$ reaction. Figure 6c (bottom) shows the molecular charges computed via Mulliken analysis for the resulting OH^+ and H_3O^+ fragments as a function of time, with four labeled points corresponding to significant events in the trajectory. Figure 6c (top) shows trajectory snapshots for each of the labeled points. Initially, the two molecules that participate in reaction are uncharged (i). Two-hole localization signified by a local charge state of +2 on a single water molecule (blue) occurs rapidly. This state is stable for ∼20 fs before the local environment becomes conducive to charge transfer. As illustrated in (ii), charge transfer occurs when an adjacent molecule (colored black) is close enough to initiate the $H_2O^{2+} + H_2O \rightarrow OH^+ + H_3O^+$ reaction. The corresponding reaction products with local charge states of +1 are illustrated in (iii). These charge states remain stable with the eventual ejection of the OH^+ fragment from the surface illustrated in (iv).

We plot similar dynamics for the bulk-like excitation in Figure 6d with the Mulliken charge dynamics for a water molecule that undergoes hole localization and splitting with 4 relevant labeled points in time. The top part of Figure 6d shows the snapshots corresponding to the labeled points. The initial uncharged molecule is illustrated in (i). At t ∼40 fs, a significant hole population on a single water molecule occurs resulting in a high charge state (+0.6), which survives for ∼20 fs. This is followed by a water splitting reaction with the formation of H_3O^+ and OH, as illustrated in (ii). This state is short-lived as rapid recombination of OH radical occurs, which is illustrated in (iii). This results in the original molecule returning to a charge-neutral state as the hole depopulates from the water molecule. The hole eventually relocalizes to the same water molecule creating a +1 charge state with the local environment illustrated in (iv). As the H_2O^+ molecule's local environment is not conducive to charge/proton transfer with other molecules, we find it ultimately escapes to the surface driven by the electric field. During the simulation, another water splitting reaction occurred prior to complete ejection of the H_2O^+ molecule (which effectively ends the simulation), resulting in H_3O^+ and H_2O^+ molecules. The final configuration is plotted in Figure S8. We see in both excitation cases that the silica surface could act as a charge donor, resulting in water splitting reactions within less than 150 fs. We find similar lifetimes of the H_2O^+ molecule when hole localization occurs in comparison to those seen in bulk water,[40,41] but note that due to the open surface, we can also see ejection of the molecule. We anticipate these dynamics will be highly dependent on the density of water molecules at the surface of the nanoparticle, as the charge transfer and dissociation are highly dependent on the local water environment.

The results illustrate that charge transfer to free molecular species plays a significant role in the catalytic activity in ionized dielectric nanoparticles. Excitations that would have led to longer charge diffusion processes in bare silica resulted in the fragmentation of the surface molecules. Due to the strong electric fields generated at the surface of the ionized nanosphere, the surface molecules' electronic states are closer to the VBM for the total system. Thus, any high-energy holes excited from the silica slab will relax into these states. In this regard, the highly ionized dielectric nanoparticle behaves analogously to a metal and can donate free hole carriers to molecular adsorbates to induce a catalytic reaction.

DISCUSSION

In conclusion, our simulations elucidate the role of electrostatically driven charge transfer and localization during strong field catalysis of SiO_2 nanoparticles. Such mechanisms have been studied in other contexts of bond fragmentation and catalysis[2−8] but have yet to be explored in strongly ionized nanosystems. Our results extend these mechanisms to strongly ionized nanosurfaces, allowing for easier interpretation of current results in the field of strong field catalysis, while also providing the ultrafast time scales on which they occur. As these mechanisms are primarily dictated by the field strength and local carrier concentration, we find that the multiscale technique introduced here will be applicable to many nanosystems with strongly ionized surfaces.

Overall, we find charge localization to be the critical limiting step for initializing bond fragmentation, which is consistent with other studies of the photodissociation of water.[40,41] In the bare wetted particle, we find primarily a threshold-like dependence on catalytic activity in terms of the global ionization field and local charge density. In strong field excitation regimes, we see extremely fast fragmentation dynamics with sub-50 fs silanol dissociation for bare surfaces and ∼100 fs charge transfer-induced water splitting when free molecules were located at the surface. While in lower-excitation regimes we did not observe fragmentation dynamics, we did see significant bond softening, which could lead to longer time reaction channels. As silica is noncatalytic prior to strong field ionization, it offers an excellent candidate for time-resolved investigations of these ultrafast dynamics. Understanding of these ultrafast dynamics is essential for not only

https://doi.org/10.1021/jacs.4c08550
J. Am. Chem. Soc. 2024, 146, 27563−27570

developing strong field catalysis but also understanding chemistry in environments with strong electrostatic fields such as in biological and astronomical chemistry. While in these cases the strong electrostatic fields are not created via strong laser excitation but via local chemical environment for biological cases[5−8,13,14] and irradiation for astronomical cases,[30] we anticipate the subsequent dynamics to be analogous to those investigated here.

■ ASSOCIATED CONTENT

Supporting Information

The Supporting Information is available free of charge at https://pubs.acs.org/doi/10.1021/jacs.4c08550.

Additional description and figures for describing the ADK simulations to compute the electric field on silica sphere ionized from 800 nm 5 fs laser pulse; additional description of the NAQMD simulations and figures describing additional supporting NAQMD simulations for the main text results (PDF)

■ AUTHOR INFORMATION

Corresponding Authors

Thomas M. Linker − *Stanford PULSE Institute, SLAC National Accelerator Laboratory, Menlo Park, California 94025, United States; Department of Physics, University of Wisconsin−Madison, Madison, Wisconsin 53706, United States;* orcid.org/0000-0002-0504-4876; Email: tlinker@slac.stanford.edu

Matthias F. Kling − *Stanford PULSE Institute, SLAC National Accelerator Laboratory, Menlo Park, California 94025, United States; SLAC National Accelerator Laboratory, Menlo Park, California 94025, United States;* Email: mfkling@slac.stanford.edu

Adam M. Summers − *Stanford PULSE Institute, SLAC National Accelerator Laboratory, Menlo Park, California 94025, United States; SLAC National Accelerator Laboratory, Menlo Park, California 94025, United States;* Email: asummers@slac.stanford.edu

Authors

Ritika Dagar − *Department of Physics, Ludwig-Maximilians-Universität Munich, D-85748 Garching, Germany*

Alexandra Feinberg − *Stanford PULSE Institute, SLAC National Accelerator Laboratory, Menlo Park, California 94025, United States*

Samuel Sahel-Schackis − *Stanford PULSE Institute, SLAC National Accelerator Laboratory, Menlo Park, California 94025, United States;* orcid.org/0000-0001-5003-9980

Ken-ichi Nomura − *Collaboratory for Advanced Computing and Simulations, University of Southern California, Los Angeles, California 90089-0242, United States;* orcid.org/0000-0002-1743-1419

Aiichiro Nakano − *Collaboratory for Advanced Computing and Simulations, University of Southern California, Los Angeles, California 90089-0242, United States;* orcid.org/0000-0003-3228-3896

Fuyuki Shimojo − *Department of Physics, Kumamoto University, Kumamoto 860-8555, Japan;* orcid.org/0000-0002-4025-0069

Priya Vashishta − *Collaboratory for Advanced Computing and Simulations, University of Southern California, Los Angeles, California 90089-0242, United States;* orcid.org/0000-0003-4683-429X

Uwe Bergmann − *Department of Physics, University of Wisconsin−Madison, Madison, Wisconsin 53706, United States;* orcid.org/0000-0001-5639-166X

Complete contact information is available at: https://pubs.acs.org/10.1021/jacs.4c08550

Notes

The authors declare no competing financial interest.

■ ACKNOWLEDGMENTS

The work at SLAC and the University of Wisconsin was supported by the U.S. Department of Energy, Office of Science, Basic Energy Sciences, Chemical Sciences, Geosciences and Biosciences Division. R.D. and M.F.K. acknowledge support from the German Research Foundation (DFG) for simulations of the strong field ionization on nanoparticles. P.V., K.N., and A.N. were supported by Office of Naval Research through a Multi-University Research Initiative (MURI) grant N00014-24-1-2313. The NAQMD simulations were performed at the Stanford Sherlock Cluster and the University of Southern California Advanced Research Computing Center.

■ REFERENCES

(1) Stark, J. Observation of the Separation of Spectral Lines by an Electric Field. *Nature* **1913**, *92* (2301), 401.

(2) Persson, B.; Avouris, P. The Effects of the Electric Field in the STM on Excitation Localization. Implications for Local Bond Breaking. *Chem. Phys. Lett.* **1995**, *242* (4−5), 483−489.

(3) Avouris, P.; Walkup, R.; Rossi, A.; Akpati, H.; Nordlander, P.; Shen, T.-C.; Abeln, G.; Lyding, J. Breaking Individual Chemical Bonds via STM-Induced Excitations. *Surf. Sci.* **1996**, *363* (1−3), 368−377.

(4) Karafiloglou, P. Control of Delocalization and Structural Changes by Means of an Electric Field. *J. Comput. Chem.* **2006**, *27* (15), 1883−1891.

(5) Adey, W. R. Biological Effects of Electromagnetic Fields. *J. Cell. Biochem.* **1993**, *51* (4), 410−416.

(6) Warshel, A.; Sharma, P. K.; Kato, M.; Xiang, Y.; Liu, H.; Olsson, M. H. Electrostatic Basis for Enzyme Catalysis. *Chem. Rev.* **2006**, *106* (8), 3210−3235.

(7) Fried, S. D.; Bagchi, S.; Boxer, S. G. Extreme Electric Fields Power Catalysis in the Active Site of Ketosteroid Isomerase. *Science* **2014**, *346* (6216), 1510−1514.

(8) Fried, S. D.; Boxer, S. G. Electric Fields and Enzyme Catalysis. *Annu. Rev. Biochem.* **2017**, *86*, 387−415.

(9) Zhou, H.-X.; Pang, X. Electrostatic Interactions in Protein Structure, Folding, Binding, and Condensation. *Chem. Rev.* **2018**, *118* (4), 1691−1741.

(10) Geissler, P. L.; Dellago, C.; Chandler, D.; Hutter, J.; Parrinello, M. Autoionization in Liquid Water. *Science* **2001**, *291* (5511), 2121−2124.

(11) Reischl, B.; Köfinger, J.; Dellago, C. The Statistics of Electric Field Fluctuations in Liquid Water. *Mol. Phys.* **2009**, *107* (4−6), 495−502.

(12) Saitta, A. M.; Saija, F.; Giaquinta, P. V. Ab Initio Molecular Dynamics Study of Dissociation of Water under an Electric Field. *Phys. Rev. Lett.* **2012**, *108* (20), No. 207801.

(13) Leoni, T.; Lelaidier, T.; Thomas, A.; Ranguis, A.; Siri, O.; Attaccalite, C.; Becker, C. On-Surface Chemistry Using Local High Electric Fields. *Nanoscale Adv.* **2021**, *3* (19), 5565−5569.

(14) Aragonès, A. C.; Haworth, N. L.; Darwish, N.; Ciampi, S.; Bloomfield, N. J.; Wallace, G. G.; Diez-Perez, I.; Coote, M. L.

Electrostatic Catalysis of a Diels−Alder Reaction. *Nature* **2016**, *531* (7592), 88−91.
(15) Shaik, S.; Danovich, D.; Joy, J.; Wang, Z.; Stuyver, T. Electric-Field Mediated Chemistry: Uncovering and Exploiting the Potential of (Oriented) Electric Fields to Exert Chemical Catalysis and Reaction Control. *J. Am. Chem. Soc.* **2020**, *142* (29), 12551−12562.
(16) Xiang, Q.; Yu, J.; Jaroniec, M. Synergetic Effect of MoS2 and Graphene as Cocatalysts for Enhanced Photocatalytic H2 Production Activity of TiO2 Nanoparticles. *J. Am. Chem. Soc.* **2012**, *134* (15), 6575−6578.
(17) Linic, S.; Aslam, U.; Boerigter, C.; Morabito, M. Photochemical Transformations on Plasmonic Metal Nanoparticles. *Nat. Mater.* **2015**, *14* (6), 567−576.
(18) Cortés, E. Activating Plasmonic Chemistry. *Science* **2018**, *362* (6410), 28−29.
(19) Wu, S.; Butt, H.-J. Near-Infrared Photochemistry at Interfaces Based on Upconverting Nanoparticles. *Phys. Chem. Chem. Phys.* **2017**, *19* (35), 23585−23596.
(20) Murdoch, M.; Waterhouse, G. I. N.; Nadeem, M. A.; Metson, J. B.; Keane, M. A.; Howe, R. F.; Llorca, J.; Idriss, H. The Effect of Gold Loading and Particle Size on Photocatalytic Hydrogen Production from Ethanol over Au/TiO2 Nanoparticles. *Nat. Chem.* **2011**, *3* (6), 489−492.
(21) Pekkanen, A. M.; DeWitt, M. R.; Rylander, M. N. Nanoparticle Enhanced Optical Imaging and Phototherapy of Cancer. *J. Biomed. Nanotechnol.* **2014**, *10* (9), 1677−1712.
(22) Xu, J.; Wu, Y.; Zhang, P.; Wu, Y.; Vallée, R. A. L.; Wu, S.; Liu, X. Resonant Scattering Manipulation of Dielectric Nanoparticles. *Adv. Opt. Mater.* **2021**, *9* (15), No. 2100112.
(23) Seiffert, L.; Henning, P.; Rupp, P.; Zherebtsov, S.; Hommelhoff, P.; Kling, M. F.; Fennel, T. Trapping Field Assisted Backscattering in Strong-Field Photoemission from Dielectric Nanospheres. *J. Mod. Opt.* **2017**, *64* (10−11), 1096−1103.
(24) Liu, Q.; Seiffert, L.; Süßmann, F.; Zherebtsov, S.; Passig, J.; Kessel, A.; Trushin, S. A.; Kling, N. G.; Ben-Itzhak, I.; Mondes, V.; Graf, C.; Rühl, E.; Veisz, L.; Karsch, S.; Rodríguez-Fernández, J.; Stockman, M. I.; Tiggesbäumker, J.; Meiwes-Broer, K.-H.; Fennel, T.; Kling, M. F. Ionization-Induced Subcycle Metallization of Nanoparticles in Few-Cycle Pulses. *ACS Photonics* **2020**, *7* (11), 3207−3215.
(25) Alghabra, M. S.; Ali, R.; Kim, V.; Iqbal, M.; Rosenberger, P.; Mitra, S.; Dagar, R.; Rupp, P.; Bergues, B.; Mathur, D.; Kling, M. F.; Alnaser, A. S. Anomalous Formation of Trihydrogen Cations from Water on Nanoparticles. *Nat. Commun.* **2021**, *12* (1), No. 3839.
(26) Seiffert, L.; Zherebtsov, S.; Kling, M. F.; Fennel, T. Strong-Field Physics with Nanospheres. *Adv. Phys. X* **2022**, *7* (1), No. 2010595.
(27) Zhang, W.; Dagar, R.; Rosenberger, P.; Sousa-Castillo, A.; Neuhaus, M.; Li, W.; Khan, S. A.; Alnaser, A. S.; Cortes, E.; Maier, S. A.; et al. All-Optical Nanoscopic Spatial Control of Molecular Reaction Yields on Nanoparticles. *Optica* **2022**, *9* (5), 551−560.
(28) Zherebtsov, S.; Fennel, T.; Plenge, J.; Antonsson, E.; Znakovskaya, I.; Wirth, A.; Herrwerth, O.; Süßmann, F.; Peltz, C.; Ahmad, I.; Trushin, S. A.; Pervak, V.; Karsch, S.; Vrakking, M. J. J.; Langer, B.; Graf, C.; Stockman, M. I.; Krausz, F.; Rühl, E.; Kling, M. F. Controlled Near-Field Enhanced Electron Acceleration from Dielectric Nanospheres with Intense Few-Cycle Laser Fields. *Nat. Phys.* **2011**, *7* (8), 656−662.
(29) Dagar, R.; Zhang, W.; Rosenberger, P.; Linker, T. M.; Sousa-Castillo, A.; Neuhaus, M.; Mitra, S.; Biswas, S.; Feinberg, A.; Summers, A. M. Tracking Surface Charge Dynamics on Single Nanoparticles. 2024, arXiv:2401.06729. arXiv.org e-Print archive. https://arxiv.org/abs/2401.06729.
(30) Tennyson, J. Spectroscopy of H3+: Planets, Chaos and the Universe. *Rep. Prog. Phys.* **1995**, *58* (4), 421.
(31) Shimojo, F.; Ohmura, S.; Mou, W.; Kalia, R. K.; Nakano, A.; Vashishta, P. Large Nonadiabatic Quantum Molecular Dynamics Simulations on Parallel Computers. *Comput. Phys. Commun.* **2013**, *184* (1), 1−8.
(32) Shimojo, F.; Fukushima, S.; Kumazoe, H.; Misawa, M.; Ohmura, S.; Rajak, P.; Shimamura, K.; Bassman Oftelie, L.; Tiwari, S.; Kalia, R. K.; Nakano, A.; Vashishta, P. QXMD: An Open-Source Program for Nonadiabatic Quantum Molecular Dynamics. *SoftwareX* **2019**, *10*, No. 100307.
(33) Shimojo, F.; Hattori, S.; Kalia, R. K.; Kunaseth, M.; Mou, W.; Nakano, A.; Nomura, K.; Ohmura, S.; Rajak, P.; Shimamura, K.; Vashishta, P. A Divide-Conquer-Recombine Algorithmic Paradigm for Large Spatiotemporal Quantum Molecular Dynamics Simulations. *J. Chem. Phys.* **2014**, *140* (18), No. 18A529.
(34) Tully, J. C. Molecular Dynamics with Electronic Transitions. *J. Chem. Phys.* **1990**, *93* (2), 1061−1071.
(35) Blöchl, P. E. Projector Augmented-Wave Method. *Phys. Rev. B* **1994**, *50* (24), 17953−17979.
(36) Perdew, J. P.; Burke, K.; Ernzerhof, M. Generalized Gradient Approximation Made Simple. *Phys. Rev. Lett.* **1996**, *77* (18), 3865−3868.
(37) Grimme, S.; Antony, J.; Ehrlich, S.; Krieg, H. A Consistent and Accurate Ab Initio Parametrization of Density Functional Dispersion Correction (DFT-D) for the 94 Elements H-Pu. *J. Chem. Phys.* **2010**, *132* (15), No. 154104.
(38) Jackson, W. B.; Amer, N. M. Direct Measurement of Gap-State Absorption in Hydrogenated Amorphous Silicon by Photothermal Deflection Spectroscopy. *Phys. Rev. B* **1982**, *25* (8), 5559−5562.
(39) Benoit, M.; Pöhlmann, M.; Kob, W. On the Nature of Native Defects in High OH-Content Silica Glasses: A First-Principles Study. *Europhys. Lett.* **2008**, *82* (5), No. 57004.
(40) Marsalek, O.; Elles, C. G.; Pieniazek, P. A.; Pluhařová, E.; VandeVondele, J.; Bradforth, S. E.; Jungwirth, P. Chasing Charge Localization and Chemical Reactivity Following Photoionization in Liquid Water. *J. Chem. Phys.* **2011**, *135* (22), No. 224510.
(41) Loh, Z.-H.; Doumy, G.; Arnold, C.; Kjellsson, L.; Southworth, S.; Al Haddad, A.; Kumagai, Y.; Tu, M.-F.; Ho, P.; March, A.; et al. Observation of the Fastest Chemical Processes in the Radiolysis of Water. *Science* **2020**, *367* (6474), 179−182.
(42) Bloch, F. Über Die Quantenmechanik Der Elektronen in Kristallgittern. *Z. Phys.* **1929**, *52* (7), 555−600.
(43) Zener, C. A Theory of the Electrical Breakdown of Solid Dielectrics. *Proc. R. Soc. London, Ser. A* **1934**, *145* (855), 523−529.
(44) Wannier, G. H. Dynamics of Band Electrons in Electric and Magnetic Fields. *Rev. Mod. Phys.* **1962**, *34* (4), 645.
(45) Linker, T. M.; Tiwari, S.; Kumazoe, H.; Fukushima, S.; Kalia, R. K.; Nakano, A.; Ramprasad, R.; Shimojo, F.; Vashishta, P. Field-Induced Carrier Localization Transition in Dielectric Polymers. *J. Phys. Chem. Lett.* **2020**, *11* (2), 352−358.

https://doi.org/10.1021/jacs.4c08550
J. Am. Chem. Soc. 2024, 146, 27563−27570